Progress In Electromagnetics Research Letters, Vol. 103, 1–6, 2022

A CMOS Compatible Broadband Ruthroff 1 : 2 TLT Balun Using Broadside-Coupled Lines and Stacked Microstrip Lines

Zeyneb Cheraiet[1, *], Mohamed T. Benhabiles[1], Tarek Djerafi[2], Farouk Grine[1], and Mohamed L. Riabi[1]

Abstract—Implementation of a broadband Ruthroff-type transmission line transformer balun with a 1 : 2 step-up impedance transformation ratio is presented in this letter. The proposed Transmission Line Transformer (TLT) balun was investigated with broadside-coupled lines using three stacked microstrip lines. The proposed balun was formed by cascading one section of modified Ruthroff-type 2 : 1 unbalanced-to-unbalanced TLT with one section of Ruthroff-type 1 : 4 TLT balun in series. The achieved fractional bandwidth of the balun is 192.17% over the frequency range from 1.2 to 6.6 GHz, which covers the IEEE 802.11 a/b/g WLAN, WiMAX applications. The measured amplitude and phase imbalances are less than 1 dB and less than 4.51°, respectively at this frequency range.

1. INTRODUCTION

Baluns have an important role in most differential RF and microwave circuits such as power amplifiers (PAs) [1], balanced mixers [2], and matching networks between antennas [3]. They are used to provide balanced outputs from an unbalanced input. The most popular transmission line balun is the Marchand balun [4]. The bandwidth of this balun is larger than that of the magnetically coupled transformer. However, two pairs of quarter wavelength transmission lines are typically used in the Marchand balun, leading to a larger occupied area. A magnetically coupled transformer has been used as a passive balun [5]. The critical issues of this kind of balun are stray inductance and the capacitance between windings which limit its upper-frequency response. Transmission line transformer (TLT) is another type of baluns. It operates by delivering energy via the transverse transmission line mode [6, 7], and its interwinding parasitics will be absorbed into the characteristic impedance of the transmission lines, resulting in a lower insertion loss and larger bandwidth than that of magnetically coupled transformer-type balun [8]. The Guanella-type TLT balun has a flexible impedance transformation ratio, which makes it utilized often in the performance of various impedance transformations [9]. However, the combination of various basic blocks to perform various impedance transformations causes higher loss within a larger area. Moreover, in the absence of ferrite materials, the magnitude difference would be greatly worsened, because of an insufficient inductance. The Ruthroff-type TLT balun allows an impedance transformation ratio of 1 : 4 using a smaller number of transmission lines than those in the Guanella-type TLT balun. In the absence of ferrite materials, it also suffers from insufficient inductance, but achieves a better magnitude difference than that of the Guanella-type TLT balun [10]. Recently, Ruthroff type balun has been revisited using CMOS and IPD technologies [10, 11], and an adjusted length of the phase compensation was utilized in those baluns to mitigate the problem of phase imbalance. Traditionally it is fabricated by bifilar windings or coaxial cables as transmission lines [12–14]. The electrical length of the Ruthroff type balun is typically less than $1/8\lambda_g$ [11], leading

Received 4 January 2022, Accepted 7 February 2022, Scheduled 14 February 2022

* Corresponding author: Zeyneb Cheraiet (zeyneb.cheraiet@umc.edu.dz).

[1] Laboratoire d'Electromagnétisme et des Télécommunications, Université des Frères Mentouri Constantine 1, Constantine, Algérie.

[2] Centre Énergie Matériaux et Télécommunications, Institut National de la Recherche Scientifique, Montreal, QC H5A1K6, Canada.

to a smaller required chip area for this balun. The applications of this balun are limited due to the disadvantage of its fixed impedance transformation ratio at 1 : 4.

In this letter, a broadband Ruthroff-type 1 : 2 TLT balun with impedance transformation from 50 Ω to 100 Ω implemented with broadside-coupled lines and stacked microstrip lines is investigated. The proposed 1 : 2 TLT balun is formed by cascading one section of Ruthroff-type 2 : 1 unbalanced-to-unbalanced TLT with one section of Ruthroff-type 1 : 4 TLT balun in series.

2. RUTHROFF 1 : 2 TLT BALUN

Four layers were stacked together to implement the Ruthroff 1 : 2 TLT balun as shown in Fig. 2(a). The used materials from the bottom to the top are Micro. 3, Micro. 2, and Micro. 1, with 127 µm thickness Rogers substrate ($\epsilon_r = 10.2$), 25.4 µm thickness Dupont substrate ($\epsilon_r = 3.4$), and 25.4 µm thickness Dupont substrate ($\epsilon_r = 3.4$), respectively. Conductors shown in pink (metal-1) and green (metal-3) are the top metal layers of micro. 1 and micro. 3, respectively, and the blue (metal-2) and violet (metal-4) colors show the bottom metal layers of micro. 1 and micro. 3, respectively. The two sections of the Ruthroff 1 : 2 TLT balun were simulated in advance to verify the performance of the two TLTs sections. To achieve broad bandwidth, the ground plane was etched in the coupled line section. The selected substrate and thickness are comparable to the CMOS die ones including the SI layer at the bottom with permittivity of 11.2 [15].

2.1. Ruthroff-Type 2 : 1 Unbalanced-to-Unbalanced TLT

As the Ruthroff topology does not support a 2 : 1 ratio, the TLT used to implement the first section of the Ruthroff 1 : 2 TLT balun is the Ruthroff 2.25 : 1 un-to-un TLT, because it has the closest impedance to the 2 : 1 [9]. Traditionally, these TLTs are realized using bifilar or trifilar windings with ferrite material [8]. Instead of these materials, a Ruthroff 1 : 2.25 TLT has been developed using both TFMS and multilayer MMIC technologies [16]. Fig. 1(a) shows the schematic diagram of the conventional 2.25 : 1 TLT [8]. This TLT includes two pairs of conductors which are connected in series on the generator side and in shunt on the other side. If the two transmission lines in Fig. 1(a) are short and ideal, the currents through the two conductors are equal and opposite. Additionally, the voltage at the beginning of the line is the same as the voltage at the end of the line [14, 17]. Therefore:

$$V_{\text{input}} - V_z = V_{\text{output}} - 0 \tag{1}$$

$$V_z - 0 = V_{\text{output}} - V_z \tag{2}$$

So the relation between V_{output} and V_{input} is: $V_{\text{output}} = 2V_{\text{input}}/3$, and if the source resistance $R_s = V_{\text{input}}/2I$. Then the load resistance,

$$RL = V_{\text{output}}/3I = 2V_{\text{input}}/9I = (4/9)(V_{\text{input}}/2I) = 4R_s/9 \tag{3}$$

Therefore the impedance transformation ratio from R_s to RL is 2.25 : 1. However, the area occupied by the conventional TLT is large because it requires two pairs of the primary and secondary windings, and to reduce the later, the modified Ruthroff 2.25 : 1 TLT shown in Fig. 1(b) was used to implement

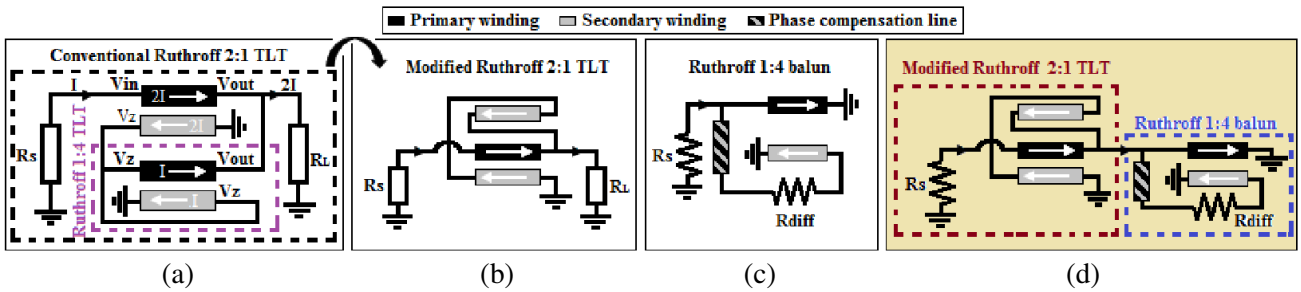

Figure 1. Schematic diagram of (a) conventional Ruthroff 2 : 1 TLT, (b) modified Ruthroff 2 : 1 TLT, (c) Ruthroff 1 : 4 TLT balun, (d) proposed Ruthroff 1 : 2 TLT balun.

the first section of the Ruthroff 1 : 2 TLT balun. In this transformer, the length of the secondary winding is twice that of the primary winding. In this way, the area of the modified TLT is about half of the conventional TLT. A spiral with one turn was utilized in the primary winding, and two turns were utilized in the spiral of the secondary winding. Metal-1 was used as the 50 Ω and 25 Ω microstrip lines, and also as the first half of the secondary winding, and the other half was implemented on metal-3. Metal-2 was used as the crossover layer and as the primary winding, and metal-4 was used as the ground plane. The primary and secondary windings were connected together in parallel and in series as shown in Figs. 2(b), (c), (d), (e) with 50.8 µm diameter vias. The same diameter via was used to connect the secondary winding with the ground plane. Table 1 lists the simulated results of the modified 2 : 1 TLT with different conductor widths. As shown in this table, the bandwidth can be increased by decreasing the metal width. Thus the largest bandwidth can be obtained with the smallest winding width.

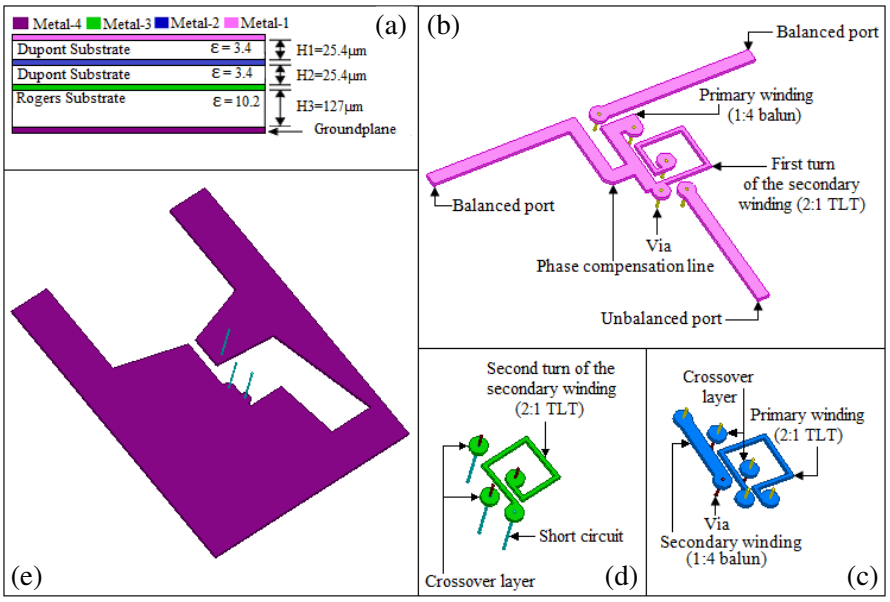

Figure 2. (a) Cross section view of the three stacked microstrip lines used to implement the proposed Ruthroff 1 : 2 balun, 3-D view of the: (b) metal 1, (c) metal 2, (d) metal 3, (e) metal 4.

Table 1. Summary of bandwidth parameters by varying the width of the broadside-coupled modified 2 : 1 TLT.

w (µm)	Feq. when $RL < -10$ dB	Feq. when $IL > -1$ dB
102	(0.67–4.86)	(0.48–5.12)
127	(0.79–4.75)	(0.58–5.10)
137	(0.84–4.72)	(0.61–5.07)
157	(0.93–4.56)	(0.70–4.96)
177	(1.02–4.47)	(0.78–4.87)

2.2. Ruthroff-Type 1 : 4 TLT Balun

Figure 1(c) shows the structure of a Ruthroff 1 : 4 TLT balun [10, 11]. The bandwidth of the balun depends on the characteristic impedance, terminated impedance, and physical length of the transmission lines [10]. The high-frequency cutoff of the Ruthroff 1 : 4 un-to-un TLT and Ruthroff 1 : 4 balun are equal [7]. In general, the characteristic impedance and length of the transmission lines command the high-frequency cutoff, and the inductance at low frequency commands the low-frequency cutoff [18].

According to the theory of the ideal coupled lines [14, 17], the impedance transformation ratio can be calculated. The currents on conductors are equal and opposite. Additionally the voltage at the beginning of the line is the same as the voltage at the end of the line. Therefore, the current that flows into the balanced ports and the voltage difference between the balanced ports are $I_{\text{input}}/2$ and $2V_{\text{input}}$, respectively. Then the impedance transformation ratio from the source impedance R_s to the balanced impedance R_{diff} is 1 : 4. The impedance transformation of the broadside-coupled Ruthroff 1 : 4 TLT balun is from 25 Ω to 100 Ω, and thus the impedance of each output port is 50 Ω. Metal-1 was used as the 25 Ω and 50 Ω microstrip lines, and also to form the primary winding and phase compensation line. Metal-2 was used as the crossover layer and to implement the secondary winding. Metals 3 was used as the crossover layers, and metal-4 was used as the ground line. 50.8 μm diameter vias were used to connect the primary and secondary windings with the ground plane (see Figs. 2(b), (c), (d), (e)). Table 2 summarizes the simulated results of the broadside-coupled Ruthroff 1 : 4 TLT balun with different metal widths. It is seen that the S_{11} bandwidth, where the return loss exceeds 10 dB, is inversely proportional to the conductor line width, but the bandwidth defined as the amplitude difference less than 1 dB is proportional to the conductor line width. In this simulation, the largest bandwidth can be obtained with the widest metal width. The metal width of the conductor line was chosen as 350 μm.

Table 2. Balun performance by varying the width of the broadside-coupled 1 : 4 TLT balun.

w (μm)	250	300	350
Feq. when Return Loss < -10 dB (GHz)	(0.31–9.39)	(0.31–7.87)	(0.31–7.75)
Feq. when Amp. Diff. $\pm$ 1 dB (GHz)	(0.01–6.67)	(0.01–6.81)	(0.01–8.01)
Feq. when Phase Diff. 180° $\pm$ 5° (GHz)	(0.01–5.75)	(0.01–10)	(0.11–10)
FCBW (%)	405.97	448.28	480

FCBW = Combined bandwidth (CBW)/center frequency (F_0); $F_0 = \text{sqrt}\,(F_l \times F_h)$. FCBW: Fractional Combined bandwidth (bandwidth with $S_{11} < -10$ dB, Amp. Diff. $\pm$ 1 dB and Phase Diff. 180° $\pm$ 5°).

3. FABRICATION AND MEASUREMENTS

To characterize the proposed Ruthroff 1 : 2 TLT balun, a combination of the two aforementioned TLTs was fabricated. Their designs and dimensions are described in the previous sections. Figs. 3(a), (b) show photographs of the chip. In this balun a 50 Ω microstrip line was connected to the input of the broadside-coupled modified Ruthroff 2 : 1 TLT, with a metal width of the primary and secondary windings of 102 μm, then the output of the broadside-coupled modified 2 : 1 TLT was connected in series with the input of the broadside-coupled Ruthroff 1 : 4 TLT balun. Both primary and secondary metal widths of the 1 : 4 TLT balun were 350 μm, and finally the endings of the phase compensation line and of the secondary winding of the 1 : 4 TLT balun were connected to a 50 Ω microstrip line, respectively. The size of the proposed balun (without the three added microstrip line access) was 2572 μm × 3257 μm. The stacked layers were fixed together. Figs. 3(c), (d) show the measured and simulated results of the proposed 1 : 2 TLT balun. In Fig. 3(c), the −10 dB S_{11} bandwidth of 5.9 GHz, which is defined as the return loss, exceeds 10 dB over the frequency range from 1.2 to 7.1 GHz. The amplitude difference is less than 1 dB from 1 to 6.6 GHz. From 1 to 6.7 GHz, the phase difference is less than 5° in Fig. 3(d). Thus the fractional combined bandwidth of 192.17% is from 1.2 to 6.6 GHz. These imbalances are calculated from the magnitude and phase responses of S_{21} and S_{31} using the following equations [19]:

$$AI = \text{dB}(S_{21}) - \text{dB}(S_{31}). \tag{4}$$

$$PI = |180^\circ - |\angle(S_{21}) - \angle(S_{31})||\,. \tag{5}$$

The measured minimum insertion loss can be derived from S_{21} and S_{31} with Equation (6) [19], and it is 0.59 dB at 2.8 GHz.

$$IL \approx -10 * \log\left(|S_{21}|^2 + |S_{31}|^2\right)\ (\text{dB}). \tag{6}$$

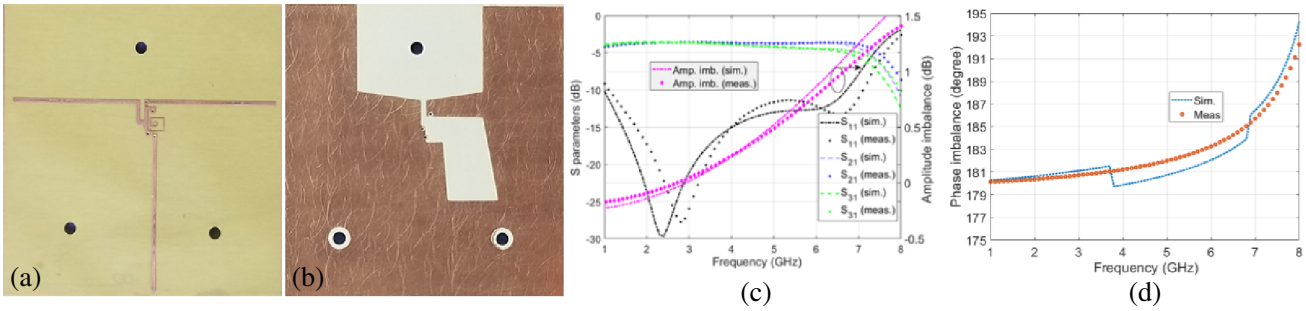

Figure 3. (a) Top view of the fabricated Ruthroff 1 : 2 TLT balun. (b) Bottom view of the fabricated Ruthroff 1 : 2 TLT balun. (c) Amplitude imbalance of the proposed Ruthroff 1 : 2 TLT balun. (d) Phase imbalance of the proposed Ruthroff 1 : 2 TLT balun.

Table 3. Comparison of the proposed balun 1 : 2 TLT balun with some recently published Marchand baluns.

Ref.	-10 dB S_{11} BW (GHz)	Imbalances Amp. (dB)/Phase (deg.)	FCBW (%)
[4]	2.39–5.68	0.35/5.26	89.40
[20]	2.28–5.41	0.42/1.81	89.17
[21]	0.6–0.88	0.65/1.20	38.53
[22]	2.14–2.64	0.19/0.84	21.01
Our work	1.2–7.1	1.15/6.07	192.17

FCBW = Combined bandwidth (CBW)/center frequency (F_0); $F_0 = \text{sqrt}\,(F_l \times F_h)$. FCBW: Fractional Combined bandwidth (bandwidth with $S_{11} < -10$ dB, Amp. Diff. $\pm$ 1 dB and Phase Diff. $180° \pm 5°$).

The simulated and measured results are in very good agreement. The slight discrepancies between the simulated and measured results are due to manufacturing including layers alignment. Table 3 compares the achieved result with published Marchand baluns. As can be seen, the proposed Ruthroff 1 : 2 TLT balun can compete against the other baluns. It outperforms on both amplitude imbalance, phase imbalance and 10 dB bandwidth.

4. CONCLUSION

A broadband Ruthroff-type 1 : 2 TLT balun with impedance transformation from 50 Ω to 100 Ω has been successfully investigated. A broadside-coupled structure was adopted using three stacked microstrip lines to obtain the large bandwidth and compact size. The ground was avoided to perform a pure coupled-mode over a broader bandwidth. The measured results show that our balun exhibits a fractional bandwidth of 192.17% over the frequency range from 1.2 to 6.6 GHz. The amplitude and phase imbalances are less than 1 dB and less than 4.51°, respectively at this frequency range.

REFERENCES

1. Niida, Y., M. Sato, T. Ohki, and N. Nakamura, "A 0.6–2.1-GHz wideband GaN high-power amplifier using transmission-line-transformer-based differential-mode combiner with second-harmonic suppression," *IEEE Transactions on Microwave Theory and Techniques*, Vol. 69, No. 3, 1675–1683, 2021.
2. Wu, Y.-C., Y.-J. Hwang, C.-C. Chiong, B.-Z. Lu, and H. Wang, "An innovative joint-injection mixer with broadband IF and RF for advanced heterodyne receivers of millimeter-wave astronomy," *IEEE Transactions on Microwave Theory and Techniques*, Vol. 68, No. 12, 5408–5422, 2020.

3. Lee, S., J. Park, and S. Hong, "Antenna switch embedded in transmission line transformers of differential PA and LNA," *IEEE Microwave and Wireless Components Letters*, Vol. 31, No. 3, 284–287, 2020.
4. Yang, Y., Y. Wu, Z. Zhuang, M. Kong, W. Wang, and C. Wang, "An ultraminiaturized bandpass filtering Marchand balun chip with spiral coupled lines based on GaAs integrated passive device technology," *Journal Title Abbreviation*, Vol. 48, No. 9, 3067–3075, 2020.
5. Yang, G., R. Chen, and K. Wang, "A CMOS balun with common ground and artificial dielectric compensation achieving 79.5% fractional bandwidth and $< 2^\circ$ phase imbalance," *2020 IEEE/MTT-S International Microwave Symposium (IMS)*, 1319–1322, 2020.
6. Guanella, G., "New method of impedance matching in radio-frequency circuits," *The Brown Boveri Review*, Vol. 31, 125–127, 1944.
7. Ruthroff, C. L., "Some broad-band transformers," *Proceedings of the IRE*, Vol. 47, No. 8, 1337–1342, 1959.
8. Mack, R. A. and J. Sevick, *Sevick's Transmission Line Transformers: Theory and Practice*, IET, 2014.
9. Rotholz, E., "Transmission-line transformers," *IEEE Transactions on Microwave Theory and Techniques*, Vol. 29, No. 4, 327–331, 1981.
10. Chung, H.-Y., H.-K. Chiou, Y.-C. Hsu, T.-Y. Yang, and C.-L. Chang, "Design of step-down broadband and low-loss Ruthroff-type baluns using IPD technology," *IEEE Transactions on Components, Packaging and Manufacturing Technology*, Vol. 4, No. 6, 967–974, 2014.
11. Chiou, H.-K. and H.-Y. Chung, "2.5–7 GHz single balanced mixer with integrated Ruthroff-type balun in 0.18 µm CMOS technology," *Electronics Letters*, Vol. 49, No. 7, 474–475, 2013.
12. Gómez-Jiménez, P., P. Otero, and E. Márquez-Segura, "Analysis and design procedure of transmission-line transformers," *IEEE Transactions on Microwave Theory and Techniques*, Vol. 56, No. 1, 163–171, 2008.
13. Grebennikov, A., "Power combiners, impedance transformers and directional couplers," *High Frequency Electronics*, Vol. 6, No. 12, 20–38, 2007.
14. Trask, C., "Transmission line transformers: Theory design and applications," *High Frequency Electronics*, Vol. 4, 46–53, 2005.
15. Burasa, P., T. Djerafi, N. G. Constantin, and K. Wu, "On-chip dual-band rectangular slot antenna for single-chip millimeter-wave identification tag in standard CMOS technology," *IEEE Transactions on Antennas and Propagation*, Vol. 65, No. 8, 3858–3868, 2017.
16. Sobrany, R. F. and I. D. Robertson, "Ruthroff transmission line transformers using multilayer technology," *33rd European Microwave Conference Proceedings (IEEE Cat. No. 03EX723C)*, Vol. 2, 559–562, 2003.
17. Sahan, N., M. E. Inal, S. Demir, and C. Toker, "High-power 20–100-MHz linear and efficient power-amplifier design," *IEEE Transactions on Microwave Theory and Techniques*, Vol. 56, No. 9, 2032–2039, 2008.
18. Liu, S.-P., "Planar transmission line transformer using coupled microstrip lines," *1998 IEEE MTT-S International Microwave Symposium Digest (Cat. No. 98CH36192)*, Vol. 2, 789–792, 1998.
19. Huang, C.-H., T.-S. Horng, C.-C. Wang, C.-T. Chiu, and C.-P. Hung, "Optimum design of transformer-type Marchand balun using scalable integrated passive device technology," *IEEE Trans. on Components, Packaging and Manufacturing Technology*, Vol. 2, No. 8, 1370–1377, 2011.
20. Liu, X., J. Zhou, Z. Deng, and X. Luo, "Compact wideband Marchand balun with amplitude and phase compensation shield," *2019 IEEE MTT-S International Microwave Symposium (IMS)*, 448–451, 2019.
21. Ahn, H.-R. and M. M. Tentzeris, "A novel compact isolation circuit suitable for ultracompact and wideband Marchand baluns," *IEEE Transactions on Circuits and Systems II: Express Briefs*, Vol. 67, No. 10, 2299–2303, 2019.
22. Wang, Y. and J.-C. Lee, "A miniaturized Marchand balun model with short-end and capacitive feeding," *IEEE Access*, Vol. 6, 26653–26659, 2018.